Journal of Material Science and Mechanical Engineering (JMSME)
p-ISSN: 2393-9095; e-ISSN: 2393-9109; Volume 2, Issue 13; October-December, 2015 pp. 10-15

http://www.krishisanskriti.org/Publication.html

Effect of Nanoparticle Size on Natural Convection within Differentially Heated Square Enclosure Filled with Al_2O_3/Water Nanofluid

K.B. Sahu[1] and Aparna Rout[2]

[1,2]KIIT University, Bhubaneswar
E-mail: 1kbsahu@yahoo.com, [2]aparnarout@gmail.com

Abstract—*Natural convection heat transfer characteristics in a differentially heated square enclosure filled with Al_2O_3-water nanofluid is numerically studied in this work. The problem is formulated in terms of stream function-vorticity form and the resulting governing equations are discretized with finite elements using Galerkin's method. Calculations are performed for different Rayleigh numbers ($10^3 \leq Ra \leq 10^5$) and diameters of nanoparticles ($25\ nm \leq d_p \leq 100\ nm$). The influence of diameter of nanoparticles on flow pattern and temperature distribution for different Rayleigh numbers is discussed.*

1. INTRODUCTION

Natural convection flow and heat transfer within enclosure has become an important phenomenon due to its wide applications in heat exchangers, electronic cooling, engine cooling, building insulation system etc. Study of enhancement of heat transfer performance in these systems is important from energy saving point of view. The heat transfer performance in these systems can be improved by adding nano-sized particles of high thermal conductivity in the base fluid. The suspension of nanoparticles in the base fluid is known as nanofluid. Due to the addition of nanoparticles, thermal conductivity of fluid is demonstrated to be significantly higher than the base fluid [1]. These nanofluids can be considered as a single phase fluid where both the fluid phase and solid nanoparticles are in thermal equilibrium. Recently nanotechnology has become one of the most important and exciting field of engineering and technology and it appears promising to give a new direction to technological advancement. Many research have been carried out for natural convection in enclosures where the increase in heat transfer rate with increasing volume fraction of nanoparticles is reported [2, 3]. Oztop & Abu-Nada [4] studied the natural convection in partially heated rectangular enclosure filled with (Cu, Al_2O_3 & TiO_2)/water nanofluids and investigated the effect of volume fraction of nanoparticles on fluid flow and temperature field.

Recently, Kefayati et al. [5] investigated natural convection in enclosure using nanofluid of temperature dependent thermophysical properties. They observed that the Nusselt number first increases as Ra is increased from 10^3 to 10^4 and then decreases as Ra is increased from 10^4 to 10^5. But by considering constant properties of nanofluids, Nu was found to increase with increase in Ra in the range 10^3 & 10^6 as reported by Lai & Yang [6]. The nanofluids with variable thermal conductivity and viscosity have been studied by Abu-Nada [7] for enclosures having various aspect ratios, where the enclosures having high aspect ratios showed more deterioration in the average Nusselt number than that of enclosures having low aspect ratios. Several other investigations have also been carried out with varying width to height aspect ratio. Corcione [8] observed that enclosures with high aspect ratios showed more deterioration in average Nu than that for enclosures having low aspect ratios. C. Lin & Violi [9] investigated the effect of non-uniform particle diameter on thermal conductivity in differentially heated enclosure. They observed that the heat transfer characteristics were enhanced with decrease in mean nanoparticle diameter. In the present work, the effect of nanoparticle size on flow and heat transfer characteristics in square enclosures has been studied.

2. ANALYSIS

Fig. 1 shows the schematic of the square enclosure considered for this study. The enclosure having length L containing Al_2O_3/water nanofluid is differentially heated at the side walls while the top and bottom walls are insulated. The left and the right vertical walls are kept at high and low temperature respectively. No slip condition is employed at all the walls. The nanofluid is considered as Newtonian, incompressible and the nanoparticles are assumed to have uniform shape and size.

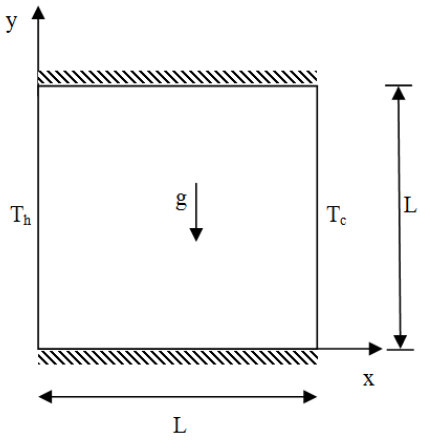

Fig. 1: Sketch of problem geometry and coordinate system

The flow of nanofluid inside the enclosure is considered to be laminar. The nanofluid is assumed to behave like a single phase fluid with its effective properties as temperature dependent. Boussinesq approximation is employed for gravity terms in the momentum conservation equation. Based on these assumptions, the governing equations are written in dimensional form as follows:

Continuity equation

$$\frac{\partial^2\psi}{\partial x^2}+\frac{\partial^2\psi}{\partial y^2}=-\omega \tag{1}$$

Momentum equation

$$u\frac{\partial\omega}{\partial x}+v\frac{\partial\omega}{\partial y}=\nu_{nf}\nabla^2\omega+g\beta\frac{\partial T}{\partial x} \tag{2}$$

Energy equation for constant fluid properties without internal heat generation, and negligible viscous dissipation

$$u\frac{\partial T}{\partial x}+v\frac{\partial T}{\partial y}=\alpha\left[\frac{\partial^2 T}{\partial x^2}+\frac{\partial^2 T}{\partial y^2}\right] \tag{3}$$

By using the following dimensionless variables,

$$X=\frac{x}{L},Y=\frac{y}{L},U=\frac{u}{\mu_r/\rho_r L},V=\frac{v}{\mu_r/\rho_r L},\theta=\frac{T-T_c}{T_h-T_c},$$

$$\Omega=\frac{\omega L}{\mu_r/\rho_r L},\Psi=\frac{\psi}{\mu_r/\rho_r} \tag{4}$$

The governing equations can be written in non-dimensionalised form as

$$\frac{\partial^2\Psi}{\partial X^2}+\frac{\partial^2\Psi}{\partial Y^2}=-\Omega \tag{5}$$

$$U\frac{\partial\Omega}{\partial X}+V\frac{\partial\Omega}{\partial Y}=Pr\,\nabla^2\Omega+\mathrm{Pr}\,Ra\frac{\partial\theta}{\partial x} \tag{6}$$

$$U\frac{\partial\theta}{\partial X}+V\frac{\partial\theta}{\partial Y}=\nabla^2\theta \tag{7}$$

The dimensionless boundary conditions are

On the left wall i.e. X=0,

$$\Omega_{i,j}=\frac{-2(\Psi_{i,j+1}-\Psi_{i,j})}{(\Delta X)^2},\ \Psi=0,\ \theta=1$$

On the right wall i.e. X=1,

$$\Omega_{i,j}=\frac{-2(\Psi_{i,j+1}-\Psi_{i,j})}{(\Delta X)^2},\ \Psi=0,\ \theta=0$$

On the top and bottom walls i.e. Y=0 and Y=1,

$$\Psi=0,\ \Omega_{j,i}=\frac{-2(\Psi_{i,j+1}-\Psi_{i,j})}{(\Delta Y)^2},\ Q=0$$

(where, i, j represents a point on the wall, and i, j+1 represents a point on an adjacent layer at a distance Δy from the wall [4])

The equations for temperature-dependent thermophysical properties of water [17] and Al_2O_3 [18] are incorporated in the numerical procedure and the nanofluid effective properties are calculated [10, 11, 12, 13, 16] as

$$\frac{k_{nf}}{k_f}=1+4.4Re^{0.4}Pr_f^{\,0.66}\left(\frac{T}{T_{fr}}\right)^{10}\left(\frac{k_s}{k_f}\right)^{0.03}\phi^{0.66} \tag{8}$$

Where, T_{fr} is the freezing point temperature of water.

$$\frac{\mu_{nf}}{\mu_f}=\frac{1}{1-34.87(d_p/d_f)^{-0.3}\phi^{1.03}} \tag{9}$$

$$\rho_{nf}=\phi\rho_s+(1-\phi)\rho_f \tag{10}$$

$$C_{nf}=\frac{(1-\phi)(\rho C)_f+\phi(\rho C)_s}{(1-\phi)\rho_f+\phi\rho_s} \tag{11}$$

$$Ra=Ra_f\frac{(\rho/\rho_f)_r\,(C/C_f)_r}{(k/k_f)_r\,(\mu/\mu_f)_r}\times\frac{\rho_c-\rho_h}{(\rho_f)_c-(\rho_f)_h} \tag{12}$$

$$Pr=Pr_f\frac{(C/C_f)_r\,(\mu/\mu_f)_r}{(k/k_f)_r} \tag{13}$$

3. NUMERICAL PROCEDURE AND CODE VALIDATION

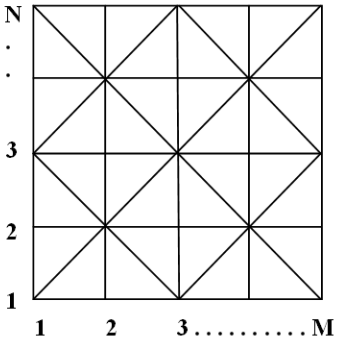

Fig. 2: Computational domain with mesh pattern

The governing equations are solved by finite-element method. The computational domain is represented by (M × N) nodes and 2(M-1) × (N-1) linear triangular elements as shown in Fig. 2. All the governing equations for mass, momentum and energy are numerically discretized in the computational domain using above mentioned triangular elements. The equations are developed first by using Galerkin's method and

then assembled in order to get equations for whole computational domain. The necessary boundary conditions: isothermal walls along y-direction and insulated walls along x-direction are imposed, which modifies both the conductivity matrix and heat rate vector appropriately. Initially, the nodal temperatures are obtained by assuming only conduction. At element temperature, the effective Ra and Pr are calculated (Eq. 12, Eq. 13). Taking these values, the momentum equation is solved to find the vorticity at each nodal point. The vorticity, thus obtained, is used to solve the continuity equation. So the values of stream function at each node are obtained. From the stream function values, the velocity field is updated. Then the energy conservation equation for convection is solved to find the updated temperature field. The various properties of nanoparticle, base fluid and nanofluid are calculated at the updated temperature with the same procedure discussed earlier. Then the updated temperature and velocity field are again used to solve the momentum equation for updating the vorticity at each node. Due to the interlocking of various equations as well as boundary conditions, an iterative process is needed for obtaining the numerical solution. This iterative procedure is continued till the convergence is obtained (i.e. $\theta^{n+1} - \theta^{n} < 10^{-5}$); where n+1 and n signify two consecutive levels of iteration. The author experienced during the investigation that under-relaxation of momentum and energy equations are required for obtaining convergence. The Nusselt number at hot and cold side walls are obtained by following expressions.

$$Nu_h = \frac{Q_h}{k(T_h - T_c)} = \int_0^1 \frac{\partial \theta}{\partial x}\Big|_{x=0} dY \quad (14)$$

$$Nu_c = \frac{Q_c}{k(T_h - T_c)} = \int_0^1 \frac{\partial \theta}{\partial x}\Big|_{x=1} dY \quad (15)$$

It has been found during investigation that, the average Nusselt number at the hot and cold walls is the same, which is taken as the average Nusselt number for the enclosure.

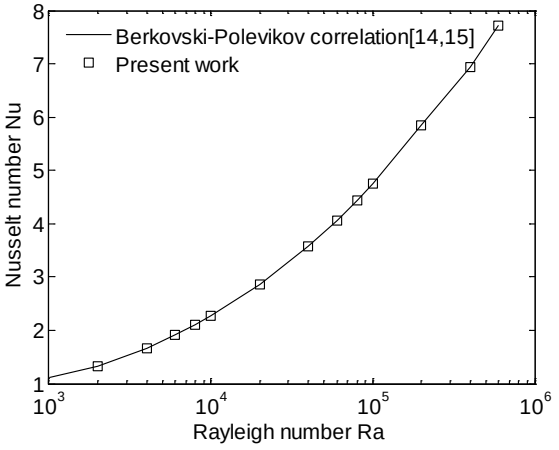

Fig. 3: Comparison between present work and Berkovski-Polevikov correlation

Grid-independence test is carried out to choose a suitable grid size for all calculations. Results for ϕ=0.01, d_p=25 nm, T_c=303 K, T_h=313 K and Ra_f=10^4 and 10^5 with different grids of 16×16, 20×20, 24×24, 28×28 and 32×32 are obtained. As the grid size is changed from 28×28 to 32×32, no remarkable variation in the results is observed.

The computational procedure is validated by comparing the average Nu computed by the present code for different Ra with the Berkovski-Polevikov correlation [14, 15] which is based on experimental and numerical data for laminar natural convection of water in a square cavity differentially heated at sides. The results obtained by the present code are in very good agreement with the Berkovski-Polevikov correlation (Fig. 3). The accuracy of the solution tested from the energy balance of the cavity and validation of the code as described above does not encourage the authors to work with higher than 32×32 grid size.

4. RESULTS AND DISCUSSION

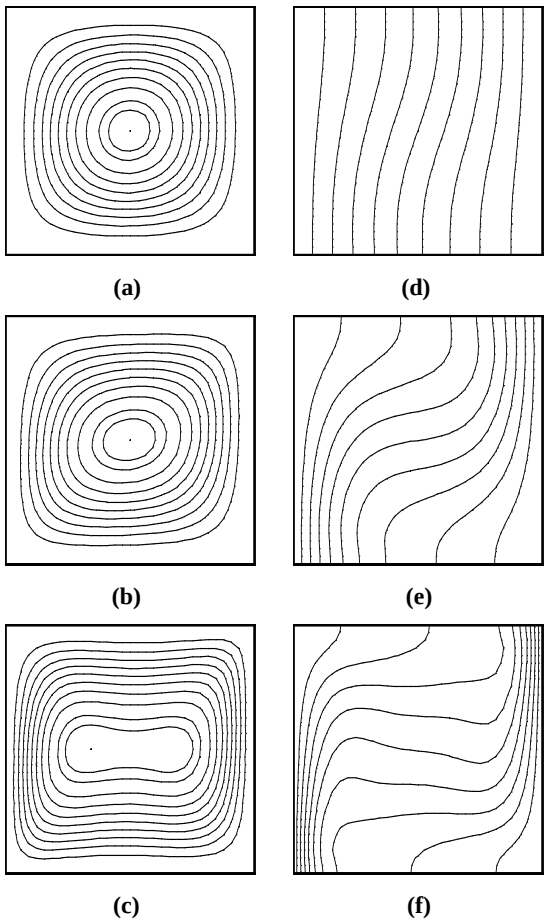

Fig. 4: Effect of Ra on the isotherm and streamline contour plots for ϕ=0.04 T_c =313 K, ΔT=10 K and d_p=25nm.

Numerical calculations are performed for different values of Ra_f (10^3-10^5), d_p (25 nm-100 nm), T_h (303 K-323 K) and the T_c (293 K-313 K). The contour lines of isotherm and constant

stream function plots correspond to equally spaced values of θ and $(\Psi/\Psi max)$ in the range between 1 and 0. The results may be analyzed and discussed as follows.

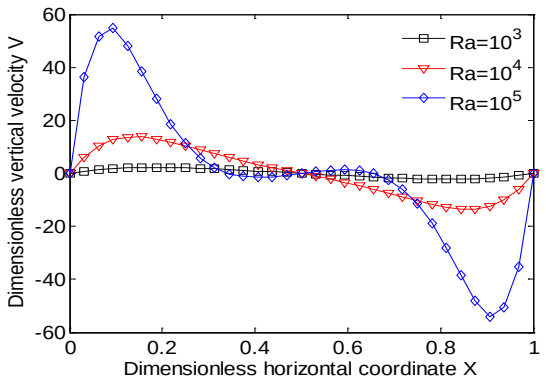

Fig. 5: Distribution of (a) V vs X along horizontal mid-plane and (b) U vs Y along vertical mid-plane (d_p =25 nm, T_c=313 K, ϕ=0.04)

4.1. Effect of Rayleigh number

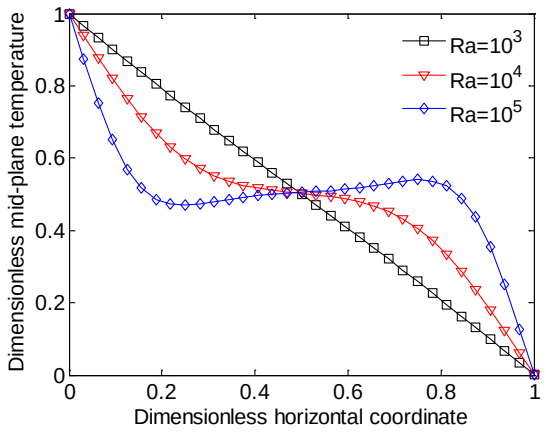

Fig. 6: θ vs X along horizontal mid-plane with Ra as a parameter at T_c=313 K and ϕ=0.04

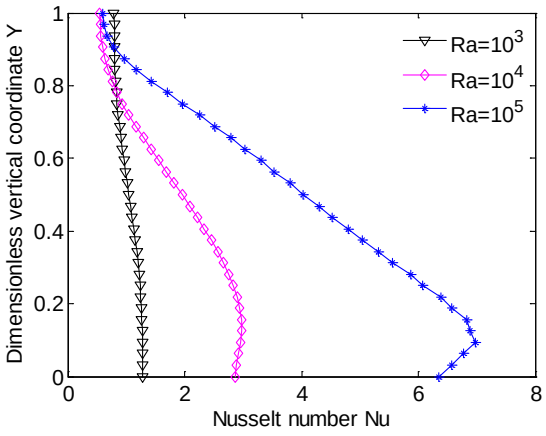

Fig. 7: Variation of Nu along hot wall with different Ra (ϕ=0.04, Tc=313 K, d_p =25 nm)

When hot and cold wall temperatures, size and concentration of nanoparticles remain same, increase in Rayleigh number implies increase in the enclosure size. So, higher Rayleigh number results in higher buoyancy effect. For low Rayleigh number (Ra_f =10^3), convection is negligible due to less buoyancy effect and the fluid circulation rate is very low within the enclosure (Fig. 4 (a)). As Ra increases, the fluid circulates at higher rate due to increased buoyancy effect which is observed from the streamline contour plots (Fig. 4 (b) and (c)). For bigger enclosure (Ra=10^5), the extent of heat diffusion between the vertical active walls and the adjacent fluid is not up to the core. So the flow of fluid moves vertically near these walls and the core remains stagnant. The vertical velocity component of fluid along horizontal mid-plane (Fig. 5) corroborates this. Then the fluid leaves the active walls and moves along the insulated horizontal walls. As there is no heat interaction of the fluid with the insulated horizontal walls, the fluid spreads out from the wall up to the core region. The distribution of streamlines also shows this. The heat transfer between hot and cold walls takes place mainly by conduction at lower Rayleigh number for which the isotherms are almost vertical (Fig. 4 (d)). But for higher Rayleigh numbers, the isotherms are more curved because of more convection effect (Fig. 4 (e) and (f)). As the heat transfer mechanism changes from conduction to convection, the isotherms are more compressed towards the wall and hence higher temperature gradient is observed near the hot and cold walls (Fig. 6).

Fig. 7 shows the variation of local Nusselt number along the hot wall for various Rayleigh numbers. The cold fluid first interacts the hot wall at its bottom. Since the temperature difference between the wall and fluid is more, the heat transfer is more at the bottom of the hot wall. The temperature of the fluid is increased gradually as it receives more heat while moving upward and the temperature difference between the wall and fluid is decreased. So the Nusselt number is less at the upper portions of the hot wall compared to its bottom portion. Barring the uppermost region, the Nusselt number at any other location of the hot wall is more for higher Rayleigh number as the convection is more. For bigger enclosure, the fluid at the top portion of the hot wall is almost stagnant due to sudden change of direction at the corner. But for smaller enclosure, the fluid flows in to the corner portion at low velocities.

4.2. Effect of nanoparticle diameter

Fig. 8 shows the streamlines and isotherm contours for nanofluids with different nanoparticle sizes with same Rayleigh number and volume fraction. From Fig. 8 (a), it is observed that the streamlines are compressed towards the walls in case of larger particle diameter, which represents strengthening of flow of fluid inside the enclosure. The

distribution of vertical component of velocity (Fig. 9) illustrates the same. This is because with same volume fraction when particle diameter increases, the number of nanoparticles becomes less. So with increase in particle size the number of collisions between nanoparticles is reduced, which results in decrease in viscosity of the nanofluid. Due to higher circulation of fluid with increase in nanoparticle diameter, the isotherms are also compressed towards the walls as observed from Fig. 8 (b). So, the temperature gradient near the walls increases with increase in nanoparticle size (Fig. 10).

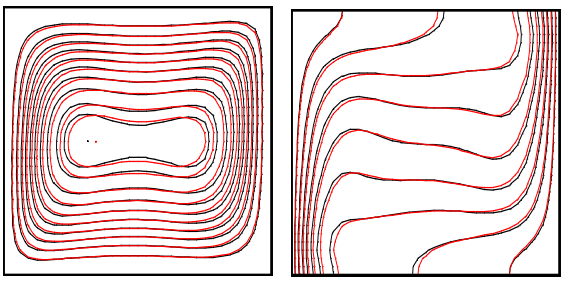

Fig. 8: Effect of the nanoparticle diameter on the (a) isotherm and (b) streamline contour plots for Ra=10^5, T_c=313 K, ΔT=10 K, ϕ=0.04

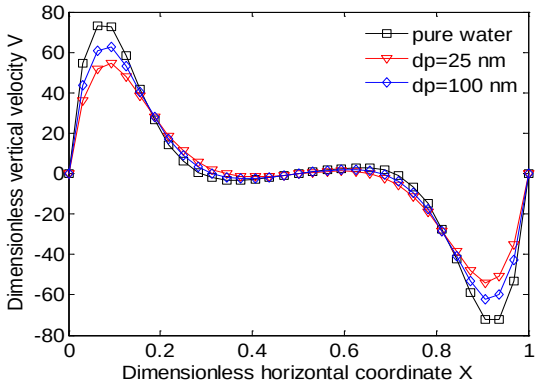

Fig. 9: Distribution of V vs X along horizontal mid-plane (Ra=10^5, T_c=313 K, ϕ=0.04)

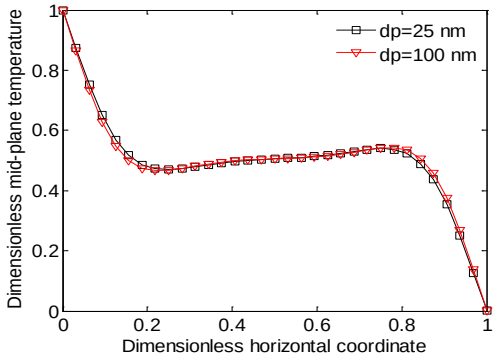

Fig. 10: θ vs X along horizontal mid-plane with dp as a parameter at T_c=313 K and ϕ=0.04

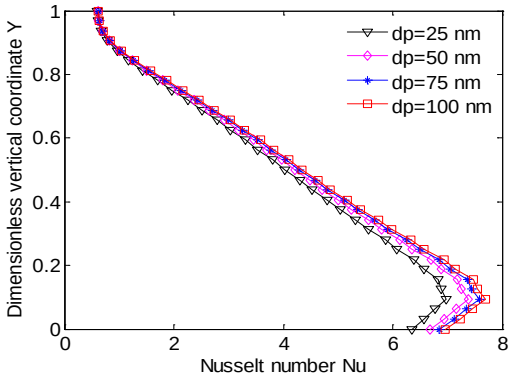

Fig. 11: Variation of Nu along hot wall with different d_p (Ra=10^5, ϕ=0.04, Tc=313 K)

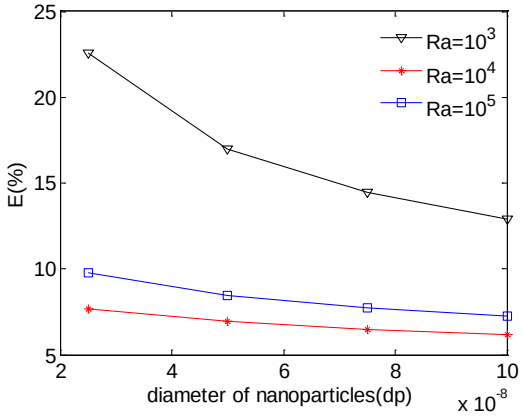

Fig. 12: E (%) vs dp for various Ra with T_c=313 K and ϕ=0.04

Fig. 11 shows the variation of Nusselt number along the hot wall for nanofluids of various nanoparticle sizes. The Nusselt number is more at the bottom portion of the wall compared to that at the top portion which has already been discussed. The Nusselt number at any location is more for nanofluids with bigger nanoparticles due to higher fluid motion.

The increase in heat transfer performance of nanofluid compared to pure base fluid is expressed in terms of heat transfer enhancement, E which is defined [10] as

$$E = \frac{h}{h_f} - 1 = \frac{Nu}{Nu_f}\left(\frac{k}{k_f}\right) - 1 \qquad (16)$$

Fig. 12 shows the variation of heat transfer enhancement with nanoparticle diameter for various Rayleigh numbers. The heat transfer enhancement is more for lower Rayleigh numbers as the conduction mode is dominant and the thermal conductivity of the nanofluid is more than the pure base fluid. But for higher Rayleigh numbers, as the convection effect dominates the conduction mode, the enhancement is more for higher Rayleigh numbers. The heat transfer enhancement is more with smaller nanoparticles for any given Rayleigh number keeping volume fraction constant.

5. CONCLUSION

Natural convection of Al_2O_3/water nanofluid inside a differentially heated square enclosure is studied numerically. Simulations have been performed for different values of Rayleigh number of the base fluid (Ra_f), in the range of 10^3-10^5, diameter of nanoparticles (d_p), in the range of 25-100 nm. The conclusion is made as follows.

- The circulation of nanofluid is more with increase in Rayleigh number keeping other parameters fixed.
- The fluid motion is higher near the active walls with core stagnant for higher Rayleigh numbers.
- The heat transfer from the active walls is more for higher Rayleigh number.
- The fluid circulation is more for bigger nanoparticle sizes keeping other parameters constant.
- The heat transfer enhancement is more effective with nanofluid compared to that with the base fluid for smaller enclosures where the heat transfer is mainly by conduction.
- The heat transfer is more for nanofluids with smaller nanoparticles keeping volume fraction constant.

REFERENCES

[1] Ho, C. J., Liu, W. K., Chang, Y. S., and Lin, C. C., "Natural convection heat transfer of alumina-water nanofluid in vertical square enclosures: An experimental study", *International journal of Thermal Sciences*, 49, 2010.

[2] Khanafer, K., Vafai, K., and Lightstone, M., "Buoyancy-driven heat transfer enhancement in a two-dimensional enclosure utilizing nanofluids", *International Journal of Heat and Mass Transfer*, 46, 2003, pp.3639-3653.

[3] Jou, R. Y., and Tzeng, S. C.," Numerical research of natural convective heat transfer enhancement filled with nanofluids in rectangular enclosures", *International Communications in Heat and Mass Transfer*, 33, 2006, pp.727-736.

[4] Oztop, H. F., and Abu-Nada, E., "Numerical study of natural convection in partially heated rectangular enclosures filled with nanofluids", *International Journal of Heat and Fluid Flow*, 29, 2008, pp.1326-1336.

[5] Kefayati, G. H. R., Hosseinizadeh, S. F., Gorji, M., and Sajjadi, H., "Lattice Boltzmann simulation of natural convection in tall enclosures using water/SiO_2 nanofluid", *International Communications in Heat and Mass Transfer*, 38, 2011, pp.798-805.

[6] Lai, F. H., and Yang, Y. T., "Lattice Boltzmann simulation of natural convection heat transfer of Al_2O_3/water nanofluids in a square enclosure", *International Journal of Thermal Sciences*, 50, 2011, pp.1930-1941.

[7] Abu-Nada, E., Masoud, Z., Oztop, H. F., and Campo, A., "Effect of nanofluid variable properties on natural convection in enclosures", *International Journal of Thermal Sciences*, 49, 2010, pp.479-491.

[8] Corcione, M., "Heat transfer features of buoyancy-driven nanofluids inside rectangular enclosures differentially heated at the sidewalls", *International Journal of Thermal Sciences*, 49, 2010, pp.1536-1546.

[9] Lin, K. C., and Violi, A., "Natural convection heat transfer of nanofluids in a vertical cavity: Effects of non-uniform particle diameter and temperature on thermal conductivity", *International Journal of Heat and Fluid Flow*, 31, 2010, pp.236-245.

[10] Cianfrini, M., Corcione, M., and Quintino, A., "Natural convection in square enclosures differentially heated at sides using Alumina-water nanofluids with temperature dependent physical properties", Eudossiana 18, 00184 Rome, Italy.

[11] Corcione, M., "Empirical correlating equations for predicting the effective thermal conductivity and dynamic viscosity of nanofluids", *Energy Conv. Manag.*, 52, 2011, pp.789-793.

[12] Keblinski, P., Phillpot, S. R., Choi, S. U. S., and Eastman, J. A., "Mechanisms of heat flow in suspensions of nano-sized particles (nanofluids)", *International Journal of Heat and Mass Transfer*, 45, 2002, pp.855-863.

[13] Pak, B. C., and Cho, Y. I., "Hydrodynamic and heat transfer study of dispersed fluids with submicron metallic oxide particles", *Exp. Heat Transfer*, 11, 1998, pp.151-170.

[14] Bejan, A., Convection Heat transfer, 3rd ed., John Wiley & Sons, Inc., Hoboken, NJ, USA, 2004.

[15] Incropera, F. P., Dewitt, D. P., Bergman, T. L., and Lavine, A. S., Fundamentals of Heat and Mass Transfer, 6th ed., John Wiley & Sons, Inc., Hoboken, NJ, USA, 2007.

[16] Xuan, Y., and Roetzel, W., "Conceptions for heat transfer correlations of nanofluids", *International Journal of Heat and Mass Transfer*, 43, 2000, pp.3701-3707.

[17] Mostafa, H., "Thermophysical properties of sea water: a review of existing correlations and data", *MIT open access articles*, 16, 2010, pp.354-380.

[18] Thermophysical properties of high temperature solid materials, vol. 4, part 1, sec. 1, pp.8-47.